Oceanologia, 67 (1)/2025, 67101
Polish Academy of Sciences
Institute of Oceanology

https://doi.org/10.5697/JMZS3739

Vertical distribution of heterotrophic nanoflagellates in the Baltic Proper

Kasia Piwosz[1,*], Anetta Ameryk[1], Klaudia Wdówka[1], Marlena Mordec[1], Uroosa[1,2], Anastasiya Chuvakova[1], Sohrab Khan[1], Jared Vincent Lacaran[1]

Abstract
Heterotrophic nanoflagellates (HNF) are key players in marine microbial food webs, but their distribution remains poorly understood. We investigated abundance patterns of eleven HNF lineages in the Baltic Proper from May to September 2021 using Catalysed Reporter Deposition-Fluorescence In Situ Hybridisation (CARD-FISH). HNF were most abundant in surface waters, where they reached above 12,000 cells ml^{-1} in May. Median cell size varied between 3.3–4.1 µm. CRY-1 cryptophytes, Marine Stramenopiles from MAST-2 lineage, and Kathablepharidacea dominated the HNF community in surface and suboxic/sulphidic waters below the halocline. Our results make an important contribution to the understanding of HNF ecology in the Baltic Sea.

Keywords
Heterotrophic nanoflagellates; Microbial food web; Baltic Sea; Marine Stramenopiles (MAST); Cryptophytes CRY-1; Kathablepharidacea; CARD-FISH; Fluorescence in situ hybridisation

[1]*Department of Fisheries Oceanography and Marine Ecology, National Marine Fisheries Research Institute, Kołłątaja 1, 81–332 Gdynia, Poland*
[2]*Institute of Oceanology of Polish Academy of Sciences, Sopot, Poland*
***Correspondence**: kpiwosz@mir.gdynia.pl

Received: 14 August 2024; **revised:** 29 October 2024; **accepted**: 6 November 2024

1. Introduction

Baltic is one of the largest brackish seas in the world. Unique geographical conditions create steep horizontal and vertical gradients of salinity, with profound consequences for its inhabitants (Herlemann et al., 2011; Hu et al., 2016; Telesh et al., 2011). Vertical salinity gradient, ranging from 7 to > 12 in the Baltic Proper, prevents deeper mixing of the water column, creating hypoxic (oxygen concentration < 2 mg l^{-1}) to sulphidic zones below the halocline at 60–80 m. The re-oxygenation of deep layers requires inflows of saline, oxygenated surface water from the North Sea that sinks and flows eastwards close to the bottom. The presence of hypoxic zones is a natural phenomenon in the Baltic but their area is expanding due to the decay of intense, eutrophication-driven cyanobacterial blooms (Zillén et al., 2008).

Microbial food webs are a key component of pelagic ecosystems. Bacteria process the majority of carbon fixed by primary producers in the ocean (review by Azam and Malfatti (2007)). In the Baltic Sea, this number ranges from < 2% to 80%, depending on the time of year (Ameryk et al., 2005; Witek et al., 1997). Bacterial production is channelled to higher trophic levels mostly via heterotrophic flagellated protists, with cell size 2–20 µm (heterotrophic nanoflagellates: HNF) that feed on bacteria while being themselves prey for microzooplankton (Azam et al., 1983; Azam and Malfatti, 2007).

HNF have almost no characteristic morphology: they are small, oval cells with two flagella. Therefore, their diversity was unrecognized until the application of molecular methods (Lopez-Garcia et al., 2001; Moon-van der Staay et al., 2001). The rapid development of high-throughput sequencing techniques has accelerated our knowledge of protist diversity in marine environments (de Vargas et al., 2015; Guillou et al., 2013; Tedersoo et al., 2024). In the Baltic Sea, previously unreported groups have been discovered (Mazur-Marzec et al., 2024). As in the case of larger protists (Telesh et al., 2013; Telesh et al., 2011), HNF communities were shown to be structured by environmental gradients in the Baltic Sea, with salinity being the dominant factor both at large and local scales (Hu et al., 2016; Piwosz et al., 2018).

However, amplicon sequencing methods do not allow for a deeper understanding of the HNF ecology beyond community-level processes. Relative abundance from sequencing poorly corresponds with absolute cell numbers,

hampering research on the dynamics and trophic roles of HNF (Piwosz et al., 2020). These limitations can be overcome by fluorescence in situ hybridization that combines molecular methods with microscopy (Amann and Fuchs, 2008). Using specific probes that bind to rRNA in ribosomes, it is possible to visualize an HNF group of interest under a microscope and, in doing so, quantify their abundance, observe morphology and size, and even investigate food vacuole content to decipher their trophic roles (Piwosz et al., 2021). This approach enabled identification of seasonal dynamics and grazing preferences in previously unknown groups in the coastal waters of the Gulf of Gdańsk (Piwosz, 2019; Piwosz and Pernthaler, 2010, 2011) and Vistula Lagoon (Piwosz et al., 2016). However, the spatial and vertical distribution of HNF in the Baltic Sea remains poorly understood.

The aim of this study was to reveal the spatial and vertical distribution of selected HNF groups in the open Baltic Sea. We collected samples from five stations along depth profiles, from the surface to the anoxic bottom waters in early spring (May), summer (June, August) and early autumn (September). We show that HNF community in early spring is dominated by only five lineages, which may suggest low-complexity microbial food webs. Moreover, for the first time, we report HNF groups known from surface waters to be present and active under hypoxic and anoxic conditions.

2. Material and methods

2.1 Sampling

Samples were collected from the r/v *Baltica* during the statutory cruises of the National Marine Fisheries Research Institute on the following dates: 1–14 May 2021, 18–23 June 2021, 16–27 August 2021 and 13–28 September 2021 at five stations (Figure 1). Conductivity, temperature, and depth were measured using a rosette equipped with a set of twelve 5-litre Niskin bottles and the Sea-Bird SBE 911plus CTD probe. The sampling depths were selected based on the properties of the water column: surface (0–1 m), thermocline depth, halocline depth, oxycline depth and just above the bottom (Figure 2). One bottle was taken and sealed at each depth. When the depths of halocline and oxycline overlapped, another sample was taken from the depth that appeared interesting based on the vertical profiles, such as deep layers with decreased temperature and increased oxygen concentration (Figure 2). These depths were also used for oxygen measurements according to the Winkler method (Grasshoff et al., 1983). Exact sampling positions and depths are provided at Zenodo (https://zenodo.org/), DOI: https://doi.org/10.5281/zenodo.13945312.

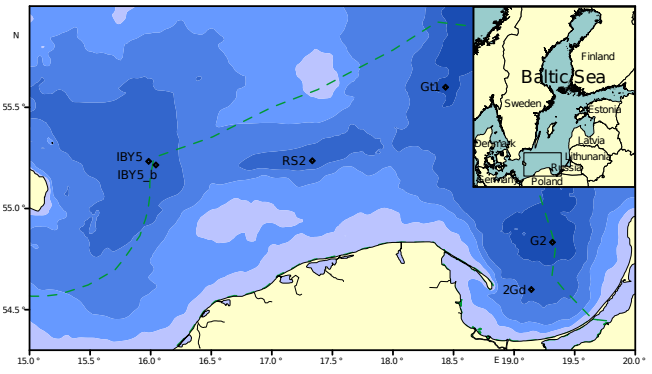

Figure 1. Map of the Baltic Sea showing location of the sampling stations.

2.2 Prokaryote abundance

10 ml of sample were fixed with particle-free formalin (Chempur, Piekary Śląskie, Poland) to a final concentration of 1%. The samples were stored in 15 ml polystyrene centrifuge tubes at 4°C in the dark until further processing. From 1 to 3.5 ml was filtered onto black polycarbonate filters (pore size 0.2 µm, diameter 25 mm, Isopore, Millipore, Burlington, USA). Cells were stained with 4′,6-diamidino-2-phenylindole (DAPI) at a concentration of 1 mg L^{-1} (Coleman, 1980) and counted at 1000× magnification under epifluorescence microscopy (Zeiss Axio Imager.M2, Jena, Germany) equipped with an LED illumination system Colibri 2 and a digital camera. Sixteen fields of view of area 14,130 μm^2 were photographed at 353 nm excitation and 465 nm emission. ACMEtool3 programme was used to count bacteria (Bennke et al., 2016).

2.3 Heterotrophic nanoflagellates abundance

A 200 ml sample was fixed with 2 ml of neutral Lugol's solution and stored in brown glass bottles at 4°C in the dark until further processing within a month. A day before filtration, particle-free formalin was added to a final concentration of 1%. Subsequently, Lugol's colourisation was removed with 4 ml of 3% $Na_2S_2O_3$, and samples were stored at 4°C in the dark for 24 h.

From 10 to 50 ml of the fixed samples were filtered onto white polycarbonate filters (pore size 0.8 µm, diameter 25 mm, Nucleopore, Whatmann, Maidstone, UK). Cells were stained with 4′,6-diamidino-2-phenylindole (DAPI) at a concentration of 1 mg L^{-1} (Coleman, 1980) and counted under an epifluorescence microscope (Zeiss Axio Imager M2) at 353 nm excitation and 465 nm emission at 1000× magnification from 20 fields of view of area 14,400 μm^2. This allowed to estimate the total abundance of nanoflagellates, without distinguishing between heterotrophic and autotrophic/mixotrophic cells. To assess the abundances of HNF only, we conducted CARD-FISH hybridization with general eukaryotic probe Euk516 (Table 1). Microphotographs were taken at 353 nm excitation and 465 nm emission for DAPI, 500/525 nm excitation/emission for probe (Alexa488) and 655/667 nm excitation/emission for autofluorescence of chlorophyll. Abundances of HNF were estimated from the proportions of hybridized cells

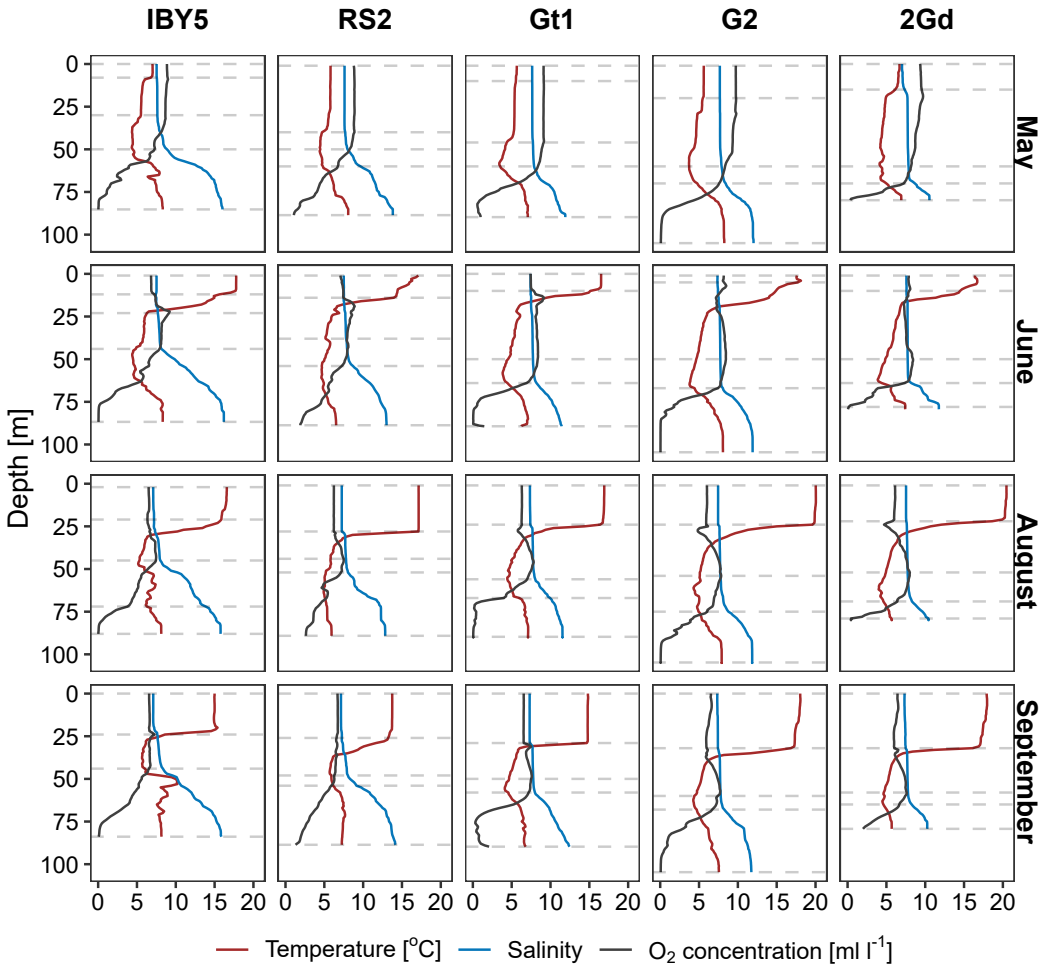

Figure 2. Vertical profiles of temperature, salinity and oxygen concentration at the sampling stations in different months.

that did not show chlorophyll autofluorescence. This approach allowed for the identification of small eukaryotic cells, whose tiny nuclei can be confused with bacterial cells.

2.4 CARD-FISH

150–190 ml were filtered onto white polycarbonate filters (pore size 0.8 µm, diameter 47 mm, Nucleopore, Whatmann), washed with 30 ml of MilliQ water, air-dried and stored at −20°C until further processing within two months. The CARD-FISH procedure followed the protocol described in Piwosz et al. (2021). Table 1 lists the used probes, along with their hybridization conditions. CARD-FISH preparations were initially screened under 400× magnification to check the quality of hybridization and to identify samples with a countable number of hybridized cells (minimum 5 cells on the whole filter piece of area 86.7 mm^2). The selected samples were counted at 1000× magnification from images taken using Zeiss Axio Imager.M2 or manually using Olympus 50×. We used 353 nm excitation and 465 nm emission for DAPI and 500/525 nm excitation/emission for probes (Alexa488). At least 100 DAPI-stained cells were evaluated in samples from the epipelagic zone, but in deep water samples, this number was difficult to reach and had to be lowered to as few as thirty cells in extreme cases. Cell size was estimated by measuring cells hybridized with the Euk516 probe from the photographs taken using a Zeiss Axio Imager.M2 and the length tool in Zen Blue software version 3.3 (Piwosz, 2019).

2.5 Design of Kath900 probe

We designed a new probe for Kathablepharidacea using the Probe_desing tool in the ARB program (Ludwig et al., 2004), as described in Piwosz et al. (2021). 1350 18S rRNA gene sequences affiliated with Cryptista were retrieved from PR2 database (version 5.0 (Guillou et al., 2013; Vaulot et al., 2022)). Sequences shorter than 900 bp were removed (756), and the remaining sequences (90% of which were > 1500 bp) were re-aligned using the MAFFT online tool with default options (Katoh et al., 2019). The alignment was trimmed using clipKIT with default gappy param-

Table 1. Probes used to target specific phylogroups of HNF. Temp – hybridization temperature. HB – formamide concentration in the hybridization buffer, Time – duration of hybridization step.

Probe	Target group	Temp [°C]	HB [%]	Time [h]	Reference
Euk516	all Eukaryotes	35	20	3	(Amann et al., 1990)
Non_Bal	none (negative control)	35	0	3	(Piwosz and Pernthaler, 2010)
Cerc02	Cercozoa	46	20	24	(Mangot et al., 2009)
CrypP1_680	CRY-1 lineage of Basal Cryptophyceae	35	40	3	(Piwosz et al., 2016)
Diplo516+C	Diplonemea	35	55	3	(Bochdansky et al., 2017)
Kath900+C	Katablepharideacea	35	55	3	this study
Kin516+C	Kinetoplastea	35	55	3	(Bochdansky and Huang, 2010)
MAST6	Sub-group II of MAST-6	35	35	3	(Piwosz and Pernthaler, 2010)
NS1A-C	MAST-1	46	30	3	(Massana et al., 2006b)
NS2	MAST-2	46	30	3	(Massana et al., 2006b)
NS3	MAST-3	46	60	3	(Massana et al., 2002)
NS4	MAST-4	46	30	3	(Massana et al., 2002)
NS7	MAST-7	35	40	3	(Giner et al., 2016)

Table 2. Sequences of the newly design probe and competitors, with information of the target group and the number of weighted mismatched (WM) based on the Test Probe online tool on Silva resource (Pruesse et al., 2007).

Probe/competitor	5′–3′ sequence	Target group/sequence	WM
Kat900 (probe)	ATAAACGCCCCCAACTATCC	Katablepharideacea	0.0
Kat900_C1	ACAAACGCCCCCAACTATCC	JQ996378	0.2
Kat900_C2	ATTAACGCCCCCAACTATCC	GU810144	1.1
Kat900_C3	ATGAACGCCCCCAACTATCC	EF526832	1.1
Kat900_C4	ATAAATGCCCCCAACTATCC	AF420478	1.5

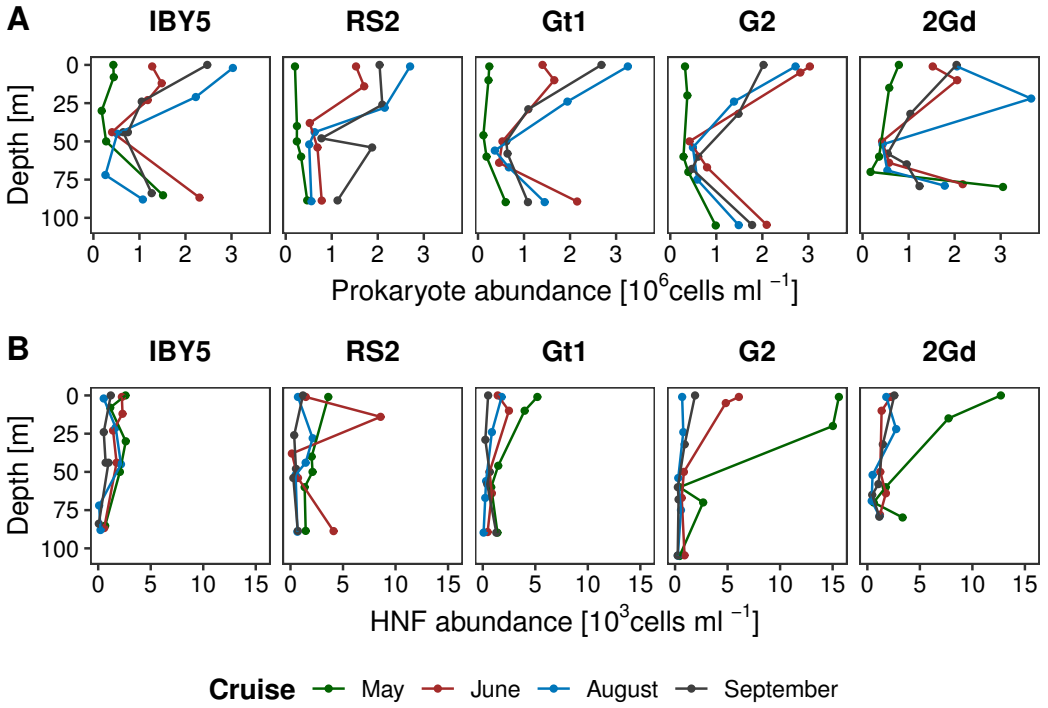

Figure 3. Vertical profiles of abundance of (A) all prokaryotes and (B) heterotrophic nanoflagellates at the sampling stations in different months.

eter set to 0.9 (Steenwyk et al., 2020). Twenty-nine sites (1.57% of the alignment) were trimmed, leaving 1817 sites (887 parsimony-informative, 342 singleton sites, 588 constant sites). The phylogenetic tree (Supplementary Figure S1) was calculated in IQ-tree with TN+F+I+G4 model automatically selected based on Bayesian Information Criterion

(Minh et al., 2020). The alignment used for tree construction, log file from the IQ-tree and the tree file in Newick format are available as Supplementary Files 1–3. The alignment and tree were then imported into ARB software and the probe was designed using the build-in Probe_design tool (Ludwig et al., 2004).

The newly designed probe Kath900 binds in the range of IV (900–910) and I (910–920) brightness class (Behrens et al., 2003). It matches more than 90% of all target sequences in the PR2 database (version 5.0) and four untargeted sequences from organisms that can be easily differentiated based on morphology: a dinoflagellate *Alexandrium* (uncultured: JN098197), two animals (uncultured Protostomia: KJ925380 and KJ925366), and one uncultured Syndiniales group I (DQ386739). There were also four sequences to which the probe had one mismatch (JQ996378, GU810144, EF526832, AF420478), for which competitors were designed (Table 2).

The hybridization conditions were initially tested in silico using the mathfish online tool (http://mathfish.cee.wisc.edu/, accessed on 17 November 2021). The results suggested that the optimal concentration of formamide in the hybridization buffer is 45% for hybridization at 35°C (Supplementary Figure S2), and that the use of competitors decreases hybridization efficiency at most to 0.75 (Supplementary Figure S3). The probe was further tested with formamide concentrations ranging from 45 to 70% with increasing step of 5% at 35°C. Approximately 200 DAPI-stained cells were counted for each condition (Supplementary Figure S4). The samples hybridized with 45 and 50% formamide displayed overly saturated signals from cells with variable cell sizes and shapes, which suggests non-specific binding. The samples hybridized with 55% formamide displayed a much higher signal-to-noise ratio and very low background fluorescence. The cells were far easier to quantify and easily distinguishable from unspecific signals and showed more uniform, spherical morphology. At higher formamide concentrations, we observed a decrease in fluorescence signal intensity until it diminished at 70% formamide. Based on these results, we decided to use 55% formamide at 35°C for further experiments (Table 1).

2.6 Data availability

All data presented in this work are available at Zenodo (https://zenodo.org/), DOI: 10.5281/zenodo.13945312.

3. Results

3.1 Hydrological conditions

The water column at all stations was well mixed in May, with constant temperature, salinity and oxygen profiles down to 50–70 m (Figure 2). The temperature was < 6°C at stations in the open waters, except for IBY5 (Bornholm Basin) and 2Gd (Gulf of Gdańsk), where it was around 7°C. Salinity was > 7.5 at all the stations except for 2Gd, where

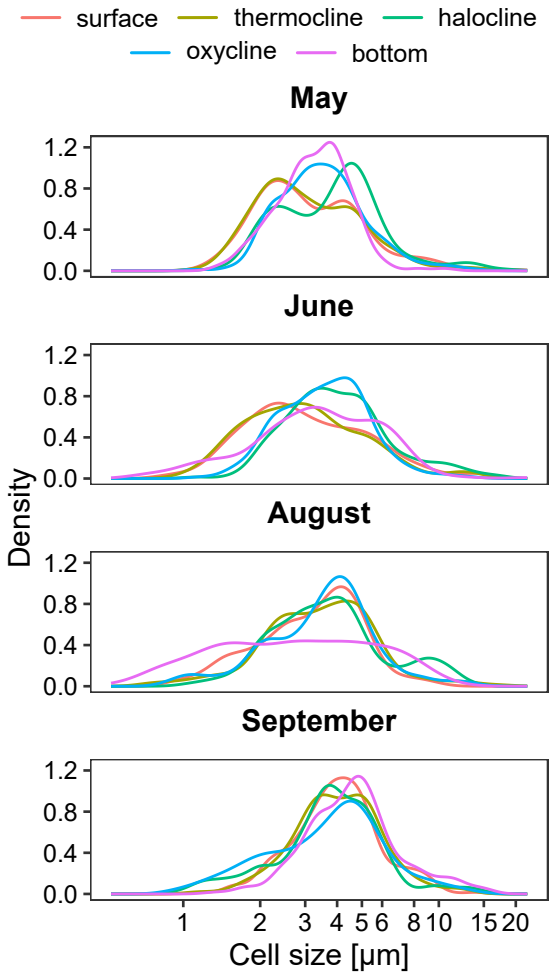

Figure 4. Size distribution of HNF in different months and depths.

it was 7. The water column was well oxygenated until thermocline and halocline, which formed below 50 m at IBY5 and 70 m at all the other stations. One meter above the bottom salinity ranged from > 10 to 16, water was warmer (> 8°C), and oxygen concentrations dropped to < 1 mg l^{-1} (Figure 2).

The conditions below 20 meters were stable throughout the remaining months, with anoxic water above the bottom (Figure 2). As the shallower water heated, a thermocline started to form in June, with temperatures gradually decreasing from about 16°C in the surface layer to < 7°C below the thermocline (about 25 m at IBY5 and 20 m at other stations). Thermocline was well developed in August, with the mixed layer reaching about 17°C in open waters and even exceeding 20°C in the Gulf of Gdańsk (stations 2Gd and G2) down to 20–30 m. Temperatures in the mixed layer decreased again to 17°C in September. Salinity was relatively stable in the mixed layers, with values > 7 at all the stations in all the months. Oxygen concentration was > 7 mg l^{-1} in June and ranged from 5.9 to 6.5 mg l^{-1} in August and from 6.0 to 7.3 in September.

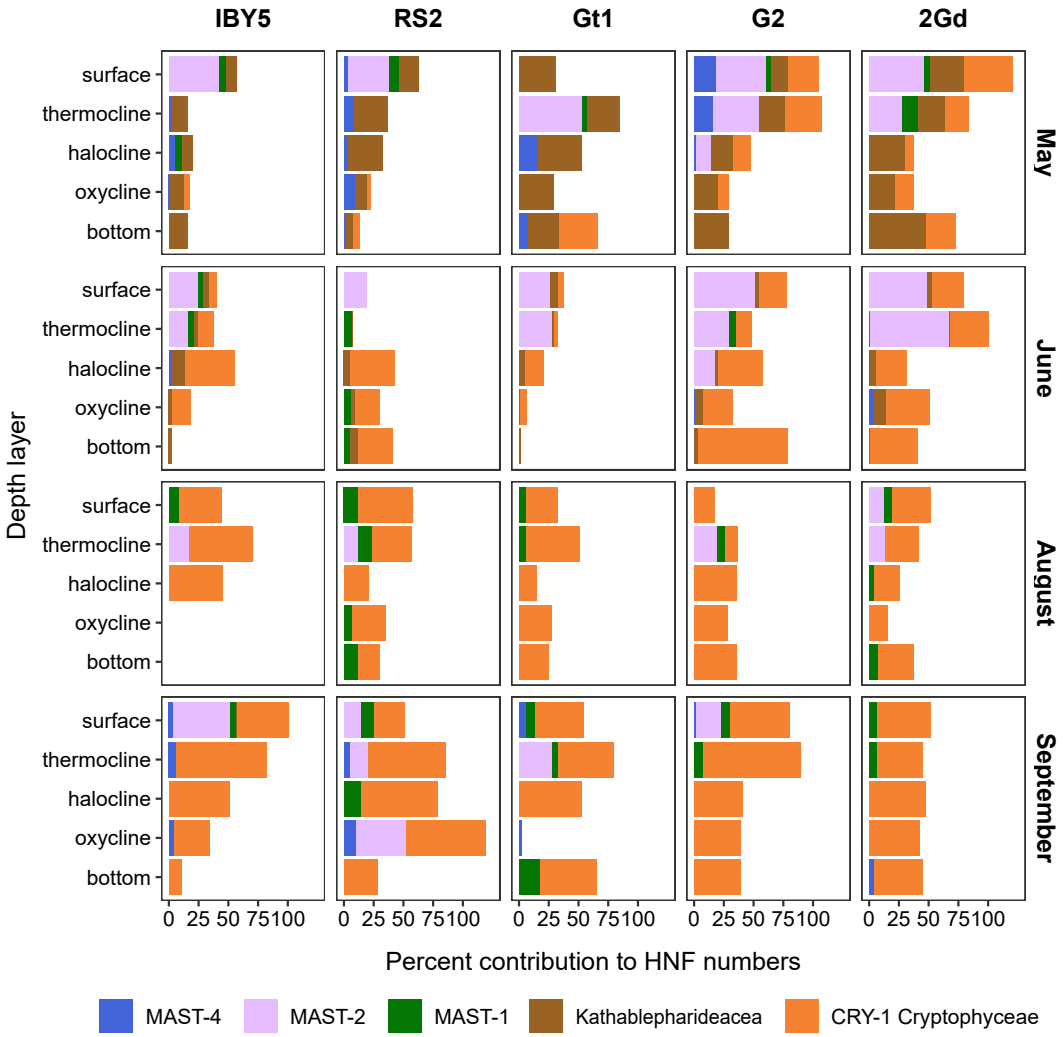

Figure 5. Percent contribution of selected HNF groups to total HNF communities along the vertical profiles at the sampling stations in different months determined using CARD-FISH.

Thermocline was between 25–30 m from June to September. Winter water masses from the previous season formed 25–50 m thick layer between the thermocline and halocline, with the coldest temperature and highest oxygen concentration. Halocline and oxycline often overlapped. Water 1 m above the bottom was anoxic or even sulphidic in summer months, with salinity ranging from 10 to 16 and temperatures between 5–10°C (Figure 2).

3.2 Abundance of prokaryotes and heterotrophic nanoflagellates

Prokaryote abundance in May did not exceed 10^6 cells ml^{-1} and varied little with depth, except for an increase just above the bottom at station 2Gd and IBY5. In other months, the vertical distribution showed an interesting pattern with a minimum at the halocline and much higher numbers in the surface and bottom waters (Figure 3A). The abundance in the surface was higher ($1.5–2.0 \times 10^6$ cells ml^{-1}) than in the bottom layer ($0.6–2.3 \times 10^6$ cells ml^{-1}). The prokaryote abundance was the lowest at halocline, where it ranged from 0.3 to 1.2×10^6 cells ml^{-1}.

In contrast to prokaryotes, HNF abundance was the highest in May, especially in the Gulf of Gdańsk (stations 2Gd and G2), where it reached $> 12 \times 10^3$ cells ml^{-1} in the surface layer (Figure 3B). HNF were less abundant ($< 5,000$ cells ml^{-1}) throughout the entire water column in other months at all stations, except for a maximum of about 8,500 cells ml^{-1} at station RS2 in June. Interestingly, at that time there was no conspicuous difference between HNF abundance in the mixed layer and below the halocline in the anoxic waters.

3.3 Size distribution of HNF

80% of HNF were smaller than 5 µm, and picoplanktonic HNF (< 3 µm) made up > 37% of all HNF (Figure 4). Only 2% of HNF were larger than 10 µm. Size distribution did

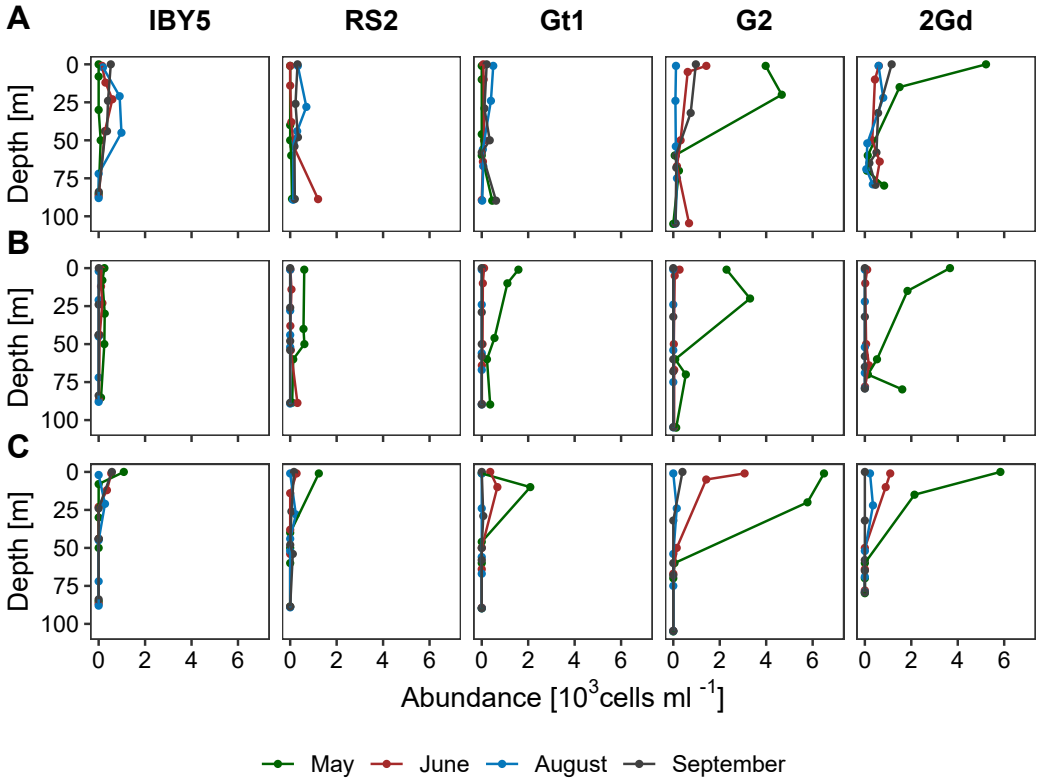

Figure 6. Vertical profiles of abundance of (A) CRY-1 cryptophytes, (B) Kathablepharidacea and (C) MAST-2 stramenopiles at the sampling stations in different months determined using CARD-FISH.

not follow the Gauss curve even after logarithmic transformation. This was especially evident in May above the halocline, where distribution was bimodal (2–3 µm and 4–5 µm, number of observations N = 1341). At halocline, a second mode included larger cells (5–6 µm). The size distribution became unimodal in deeper waters, with a median of about 4 µm at the oxycline and at 1 meter above the bottom (Figure 4). Similar patterns were observed in June and August, when cells showed bimodal distribution in surface layers and higher contribution of larger cells with depth below halocline, with an increasing median size from 3.3 µm in June (N = 1226), 3.5 µm in August (N = 1289) to 4.1 µm in September (N = 1133).

3.4 Abundance of specific HNF groups

We studied the abundance of eleven groups of HNF known to be abundant in freshwater (cercozoa from Novel Clade 2, CRY-1 cryptophytes, kathablepharids, kinetoplastids), brackish (MAST-7, MAST-6) or marine (MAST-1, MAST-2, MAST-3, MAST-4, diplonemids) environments (Table 1). Only five of these groups (MAST-1, MAST-2, MAST-4, CRY-1 and kathablepharids) were detected at higher abundances, and only three (MAST-2, CRY-1 and kathablepharids) contributed more than 20% to the total HNF numbers (Figures 5, 6). The other groups were represented only by a few cells detected during screening at lower magnification, indicating that their contribution to HNF abundance was $< 0.1\%$. Photographs of the most abundant groups are shown in Figure 7.

Bacterivorous HNF from MAST-1 and MAST-4 lineages were most abundant in May: MAST-1 reached an abundance of about 1000 cells ml^{-1} at stations G2 and 2Gd, while MAST-4 reached up to 2000 cells ml^{-1} at station 2Gd. Their abundances were close to zero in the remaining samples.

CRY-1 cryptophytes contributed the most to the HNF abundance across all depths, samples and months, making up to 50%, and even almost 75%, of all HNF (Figure 5). Their contribution increased over the season, with the lowest levels in May and the highest in September. However, their absolute abundance was the highest in May in the Gulf of Gdańsk (stations 2Gd and G2) when they reached almost 5,000 cells ml^{-1} in the layer above 20 m (Figure 6A). Except for these peaks, CRY-1 abundance was $< 1,000$ cells ml^{-1}. Interestingly, their vertical distribution varied between stations and months, with maxima found in deeper, more saline and less oxygenated or even anoxic waters just above the bottom, as observed at station RS2 in June (Figures 5, 6A).

Kathablepharids contributed most to the HNF abundance in May, when they made up around 25 to 50% of HNF at all stations except for IBY5 (Figure 5). Their con-

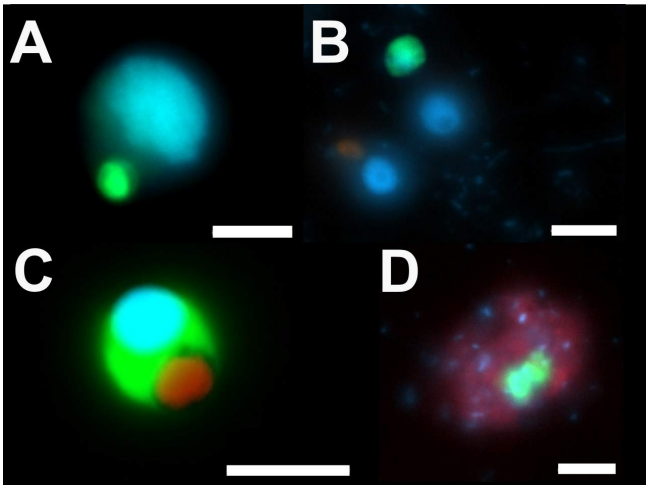

Figure 7. Microphotographs of protists hybridized with CARD-FISH. (A) a cells of heterotrophic cryptophytes from CRY-1 lineage (green) ingested by an unknown protist (blue); (B) a kathablepharid cell (green) next to two unknown protists (blue); (C) a cell of the MAST-2 stramenopile (green) with an ingested picoplankonic algae (red); (D) two cells of MAST-4 stramenopiles (green) on a particle (red with blue dots). The white bar is 5 µm wide.

tribution was generally constant along the depth, with a maximum of 50% ($> 1,600$ cells ml^{-1}) at 79 m at station 2Gd. However, their abundance varied substantially (Figure 6B). reaching maxima of over 3,000 cells ml^{-1} in the Gulf of Gdańsk (stations 2Gd and G2) in the surface layers. Their contribution was much lower in June, up to 11% at the oxycline of station 2Gd and halocline of station IBY5. Nevertheless, the highest abundance in June (300 cells ml^{-1}; 4.4% of all HNF) was observed in the surface layer at station G2. In August and September, their abundance and contribution to HNF numbers was close to the detection limit of 0.1%.

MAST-2 were the most abundant in the surface waters above the thermocline and were generally absent from more saline waters with lower oxygen concentrations, except in September at station RS2, where they contributed almost 50% of all HNF at oxycline (Figure 5). They were most abundant in May, when they reached around 6,000 cells ml^{-1} in the surface layer (Figure 6C). Their contribution was also high in June, especially in the Gulf of Gdańsk (stations 2Gd and G2), where their contribution reached 50–75% in the mixed layers, with abundance exceeding 3000 cells ml^{-1}. MAST-2 were less abundant in August and September in surface layers ($< 20\%$ and < 150 cells ml^{-1}; Figures 5 and 6C).

4. Discussion

Protists are a key component in all Earth habitats, where they play diverse roles as primary producers, parasites, and grazers (Worden et al., 2015). Unveiling their hidden diversity was made possible thanks to the development of high throughput sequencing methods, which expanded our knowledge about their ecology (de Vargas et al., 2015; Massana et al., 2015). Nevertheless, a deeper understanding of their distribution, especially along depth gradients and in anoxic waters, is still missing. In the Baltic Sea, where prokaryotic community profiles along horizontal and vertical salinity gradients have been well investigated (Bergen et al., 2014; Herlemann et al., 2011, 2014), studies of protists substantially lag behind, and almost no information is available on the diversity of heterotrophic nanoflagellates below the euphotic zone (Mazur-Marzec et al., 2024). Moreover, most information comes from amplicon-based sequencing studies, which do not provide an abundance data for the different groups (Piwosz et al., 2020). Here, we contributed to closing this knowledge gap by investigating the abundance of 11 HNF groups at 5 stations from the surface to the bottom during four months of the most productive season (May–September).

High throughput sequencing and barcoding of environmental DNA provided unprecedented insights into the diversity of microorganisms in all environments (del Campo et al., 2018; Thompson et al., 2017). Although this approach provides invaluable information about community-level processes (Logares et al., 2013; Santoferrara et al., 2020; Villarino et al., 2018), it fails to provide details on the abundance, morphology or trophic roles of detected groups. This limitation can be overcome by CARD-FISH methods but it requires design of nucleotide probes, which is not always possible (Piwosz et al., 2021). Here, we designed and optimized a new division-level probe for Kathablepharidacea (Supplementary Figure 1). Its specificity is very high, and non-target hits are from organisms with very different morphology. The probe matches sequences affiliated to other Cryptista, such as *Goniomonas*, with a minimum of two weighted mismatches, for which hybridization is unlikely to occur. The application of our new probe enabled us to obtain reliable information on the abundance of Kathablepharidacea in the Baltic Sea. Its broader use could enhance our understanding of these important microbial grazers in other habitats (Grujčić et al., 2018; Mukherjee et al., 2024).

The size distribution of the HNF community affects the structure of the food web. In general, size variance is small within a nanoflagellate species, while multimodal distribution is representative for multispecies assemblages (Piwosz, 2019). For instance, bacterivorous HNF are mostly picoplanktonic (< 3 µm) (Jürgens and Massana, 2008), while larger HNF may be omnivorous or predatory (Grujčić et al., 2018; Piwosz et al., 2021; Piwosz and Pernthaler, 2011). A bimodal size distribution at depths above the oxycline (Figure 4) indicates higher microbial food web complexity in oxygenated water compared to hypoxic or anoxic conditions, where HNF are less abundant (Figure 3),

and dinoflagellates and ciliates are the main bacterivores (Anderson et al., 2013). This interpretation is confirmed by HNF community composition, which was dominated by groups with different trophic roles in microbial food webs (Figures 5 and 6): bacterivorous MAST-1, MAST-4 and the CRY-1 lineage of cryptophytes, omnivorous Kathablepharids and predatory MAST-2 (Grujčić et al., 2018; Massana et al., 2006a).

An increase in HNF size and unimodal distribution in September may suggest a greater importance of omnivorous HNF towards the end of the season, as bacterial production decreases (Ameryk et al., 2005). Nevertheless, bacterivores remained an important part of the HNF community, as evidenced by the high contributions of CRY-1 cryptophytes at all stations (Figure 5).

Out of eleven studied HNF lineages, three groups constituted the bulk of HNF abundance over the investigated period: the bacterivorous CRY-1 lineage of cryptophytes, omnivorous Kathablepharids and predatory MAST-2. This was especially evident in May, when their combined contribution to total HNF abundance was up to 100% at certain depths (Figure 5). Considering the vast diversity of protists, especially in surface waters (Hu et al., 2016; Piwosz et al., 2018; Telesh et al., 2013), this was an unexpected finding. In contrast, the abundance diplonemids and kinetoplastids, two groups suggested to be key players in the deep ocean (Flegontova et al., 2016, 2018) were at the detection limit. These studies drew their conclusions based on amplicon sequencing, which is known to correlate poorly with actual abundances observed through microscopy (Piwosz et al., 2020). Moreover, marine diplonemids encode multiple divergent copies of 18S rRNA genes, which may inflate their contribution to amplicon reads (Mukherjee et al., 2020). Diplonemids were also found rare in deep freshwater lakes (Mukherjee et al., 2020), indicating that their environmental importance may have been overestimated. On the other hand, HNF abundance varies seasonally and their dynamics is very high (Kavagutti et al., 2023; Piwosz and Pernthaler, 2010), thus it cannot be ruled out that groups found to be rare here may be more abundant at other time points. For instance, kinetoplastids were shown to dominate in autumn in the oxygenated hypolimnion of a deep lake (Mukherjee et al., 2015). More frequent sampling campaigns are needed to fully decipher dynamics of HNF in the Baltic.

The abundances of prokaryotes and HNF generally decreased with depth (Figure 3). Such pattern of vertical distribution and the abundances has been previously reported for the Baltic Sea, where oxygen concentration is the key variable for structuring microbial communities (Anderson et al., 2012, 2013; Weber et al., 2014). Interestingly, high contributions ($>$ 20%) of kathablepharids and CRY-1 cryptophytes were observed not only in well oxygenated waters above the halocline, but also in hypoxic and anoxic waters near the bottom (Figures 2 and 5). This unexpected finding could be explained by the detection of cells sinking to the bottom (Figure 7D). However, this explanation is rather unlikely. Sinking velocities of flagellates reach up to a few centimetres per day (Lapoussière et al., 2011), meaning it would take an HNF cell about a year to sink from the surface layer to the bottom. This is much longer than the degradation time of microbial cells, which is measured in days (Strom et al., 1998). Because CARD-FISH probes bind to ribosomes and visualisation is only possible if these organelles are abundant in cells (Amann and Fuchs, 2008), dead, sinking cells would not have enough rRNA to allow for efficient hybridization to produce high fluorescence signals (Lim et al., 1999). An alternative explanation is that those signals came from species adapted to hypoxic or anoxic conditions. Kathablepharids and cryptophytes were found in deep-ocean samples (Schoenle et al., 2021) but were not detected in sulphidic waters of the Baltic and Black Seas (Wylezich et al., 2018; Wylezich and Juergens, 2011). Certainly, more research is needed on prostist ecology in oxygen deprived environments.

5. Conclusions

Here, we studied the vertical distribution of diverse groups of heterotrophic nanoflagellates (HNF) in the Baltic Sea in the productive season (May–September). We showed, for the first time, that lineages known from oxygenated waters are present in hypoxic and anoxic waters below the halocline. Based on size distribution and direct microscopic observations of multiple trophic roles in different HNF groups, we provided support for a recently amended model of food web interactions within the nanosized fraction (Piwosz et al., 2021). Finally, we designed a new probe for Kathablepharidacea.

Acknowledgements

We thank Dr Bartosz Witalis for collecting the samples in September 2021. The sampling was funded from statutory activities of the NMFRI (project DOT22/CERCOZOA). This project was funded by the National Science Centre, Poland under the Weave-UNISONO call in the Weave programme project no. 2021/03/Y/NZ8/00076.

Conflict of interest

None declared.

Supplementary materials

The authors have provided supplementary material related to this article, which can be downloaded from the following links: here and here.

References

Amann, R., Fuchs, B.M., 2008. *Single-cell identification in microbial communities by improved fluorescence in situ hybridization techniques*. Nat. Rev. Microbiol. 6, 339–348. https://doi.org/10.1038/nrmicro1888

Amann, R.I., Binder, B.J., Olson, R.J., Chisholm, S.W., Devereux, R., Stahl, D.A., 1990. *Combination of 16S ribosomal-RNA-targeted oligonucleotide probes with flow-cytometry for analyzing mixed microbial populations*. Appl. Environ. Microbiol. 56, 1919–1925. https://doi.org/10.1128/aem.56.6.1919-1925.1990

Ameryk, A., Podgorska, B., Witek, Z., 2005. *The dependence between bacterial production and environmental conditions in the Gulf of Gdansk*. Oceanologia 47, 27-45.

Anderson, R., Winter, C., Jürgens, K., 2012. *Protist grazing and viral lysis as prokaryotic mortality factors at Baltic Sea oxic–anoxic interfaces*. Mar. Ecol. Prog. Ser. 467, 1–14. https://doi.org/10.3354/meps10001

Anderson, R., Wylezich, C., Glaubitz, S., Labrenz, M., Jurgens, K., 2013. *Impact of protist grazing on a key bacterial group for biogeochemical cycling in Baltic Sea pelagic oxic/anoxic interfaces*. Environ. Microbiol. 15, 1580–1594. https://doi.org/10.1111/1462-2920.12078

Azam, F., Fenchel, T., Field, J.G., Gray, J.S., Meyer-Reil, L., Thingsted, F., 1983. *The ecological role of water-column microbes in the sea*. Mar. Ecol. Prog. Ser. 10, 257–263.

Azam, F., Malfatti, F., 2007. *Microbial structuring of marine ecosystems*. Nature Rev. Microbiol. 5, 782–791. https://doi.org/10.1038/nrmicro1747

Behrens, S., Ruhland, C., Inacio, J., Huber, H., Fonseca, A., Spencer-Martins, I., Fuchs, B.M., 2003. *In Situ Accessibility of Small-Subunit rRNA of Members of the Domains Bacteria, Archaea and Eucarya to Cy3-Labeled Oligonucleotide Probes*. Appl. Environ. Microbiol. 69, 1748–1758. https://doi.org/10.1128/AEM.69.3.1748-1758.2003

Bennke, C.M., Reintjes, G., Schattenhofer, M., Ellrott, A., Wulf, J., Zeder, M., Fuchs, B.M., 2016. *Modification of a High-Throughput Automatic Microbial Cell Enumeration System for Shipboard Analyses*. Appl. Environ. Microbiol. 82, 3289–3296. https://doi.org/10.1128/aem.03931-15

Bergen, B., Herlemann, D.P., Labrenz, M., Jürgens, K., 2014. *Distribution of the verrucomicrobial clade Spartobacteria along a salinity gradient in the Baltic Sea*. Environ. Microbiol. Rep. 6, 625–630. https://doi.org/10.1111/1758-2229.12178

Bochdansky, A., Clouse, M., Herndl, G., 2017. *Eukaryotic microbes, principally fungi and labyrinthulomycetes, dominate biomass on bathypelagic marine snow*. ISME J. 11, 362–373. https://doi.org/10.1038/ismej.2016.113

Bochdansky, A.B., Huang, L., 2010. *Re-evaluation of the EUK516 probe for the domain Eukarya results in a suitable probe for the detection of kinetoplastids, an important group of parasitic and free-living flagellates*. J. Eukaryot. Microbiol. 57, 229–235. https://doi.org/10.1111/j.1550-7408.2010.00470.x

Coleman, A.W., 1980. *Enhanced detection of bacteria in natural environments by fluorochrome staining of DNA*. Limnol. Oceanogr. 25, 948–951. https://doi.org/10.4319/lo.1980.25.5.0948

de Vargas, C., Audic, S., Henry, N., Decelle, J., Mahe, F., Logares, R., Lara, E., Berney, C., Le Bescot, N., Probert, I., Carmichael, M., Poulain, J., Romac, S., Colin, S., Aury, J.M., Bittner, L., Chaffron, S., Dunthorn, M., Engelen, S., Flegontova, O., Guidi, L., Horak, A., Jaillon, O., Lima-Mendez, G., Lukes, J., Malviya, S., Morard, R., Mulot, M., Scalco, E., Siano, R., Vincent, F., Zingone, A., Dimier, C., Picheral, M., Searson, S., Kandels-Lewis, S., Acinas, S.G., Bork, P., Bowler, C., Gorsky, G., Grimsley, N., Hingamp, P., Iudicone, D., Not, F., Ogata, H., Pesant, S., Raes, J., Sieracki, M.E., Speich, S., Stemmann, L., Sunagawa, S., Weissenbach, J., Wincker, P., Karsenti, E., Tara Oceans, C., 2015. *Eukaryotic plankton diversity in the sunlit ocean*. Science 348, 1261605. https://doi.org/10.1126/science.1261605

del Campo, J., Kolisko, M., Boscaro, V., Santoferrara, L.F., Nenarokov, S., Massana, R., Guillou, L., Simpson, A., Berney, C., de Vargas, C., Brown, M.W., Keeling, P.J., Wegener Parfrey, L., 2018. *EukRef: Phylogenetic curation of ribosomal RNA to enhance understanding of eukaryotic diversity and distribution*. PLoS Biol. 16, e2005849. https://doi.org/10.1371/journal.pbio.2005849

Flegontova, O., Flegontov, P., Malviya, S., Audic, S., Wincker, P., de Vargas, C., Bowler, C., Lukeš, J., Horák, A., 2016. *Extreme diversity of diplonemid eukaryotes in the ocean*. Curr. Biol. 26, 3060–3065. https://doi.org/10.1016/j.cub.2016.09.031

Flegontova, O., Flegontov, P., Malviya, S., Poulain, J., de Vargas, C., Bowler, C., Lukeš, J., Horák, A., 2018. *Novel marine kinetoplastids are dominant kinetoplastids in the global ocean*. Environ. Microbiol. 20, 878–889. https://doi.org/10.1111/1462-2920.14034

Giner, C.R., Forn, I., Romac, S., Logares, R., de Vargas, C., Massana, R., 2016. *Environmental sequencing provides reasonable estimates of the relative abundance of specific picoeukaryotes*. Appl. Environ. Microbiol. 82, 4757–4766. https://doi.org/10.1128/aem.00560-16

Grasshoff, K., Ehrhardt, M., Kremling, K., 1983. *Methods for sea water analysis*. Verlag Chemie GmbH, 419 pp.

Grujčić, V., Nuy, J.K., Salcher, M.M., Shabarova, T., Kasalický, V., Boenigk, J., Jensen, M., Šimek, K., 2018. *Cryptophyta as major bacterivores in freshwater summer plankton*. ISME J. 12, 1668–1681.

https://doi.org/10.1038/s41396-018-0057-5

Guillou, L., Bachar, D., Audic, S., Bass, D., Berney, C., Bittner, L., Boutte, C., Burgaud, G., de Vargas, C., Decelle, J., del Campo, J., Dolan, J.R., Dunthorn, M., Edvardsen, B., Holzmann, M., Kooistra, W., Lara, E., Le Bescot, N., Logares, R., Mahe, F., Massana, R., Montresor, M., Morard, R., Not, F., Pawlowski, J., Probert, I., Sauvadet, A.L., Siano, R., Stoeck, T., Vaulot, D., Zimmermann, P., Christen, R., 2013. ThePROTISTRIBOSOMALREFERENCEDATABASE(PR2):ACATALOGOFUNICELLULAREUKARYOTESMALLSUB-UNITRRNASEQUENCESWITHCURATEDTAXONOMY. Nucleic Acids Res. 41, D597–D604.
https://doi.org/10.1093/nar/gks1160

Herlemann, D.P.R., Labrenz, M., Juergens, K., Bertilsson, S., Waniek, J.J., Andersson, A.F., 2011. *Transitions in bacterial communities along the 2000 km salinity gradient of the Baltic Sea*. ISME J. 5, 1571–1579.
https://doi.org/10.1038/ismej.2011.41

Herlemann, D.P.R., Woelk, J., Labrenz, M., Jürgens, K., 2014. *Diversity and abundance of "Pelagibacterales" (SAR11) in the Baltic Sea salinity gradient*. Syst. Appl. Microbiol. 37, 601–604.
https://doi.org/10.1016/j.syapm.2014.09.002

Hu, Y.O.O., Karlson, B., Charvet, S., Andersson, A.F., 2016. *Diversity of pico- to mesoplankton along the 2000 km salinity gradient of the Baltic Sea*. Front. Microbiol. 7, 679.
https://doi.org/10.3389/fmicb.2016.00679

Jürgens, K., Massana, R., 2008. *Protistan grazing in marine bacterioplankton*. [In:] Kirchman, D.L. (Ed.), *Microbial Ecology of the Oceans*. Wiley-Blackwell, New Jersey, 383–441.

Katoh, K., Rozewicki, J., Yamada, K.D., 2019. *MAFFT online service: multiple sequence alignment, interactive sequence choice and visualization*. Brief Bioinform. 20, 1160–1166.
https://doi.org/10.1093/bib/bbx108

Kavagutti, V.S., Bulzu, P.-A., Chiriac, C.M., Salcher, M.M., Mukherjee, I., Shabarova, T., Grujčić, V., Mehrshad, M., Kasalický, V., Andrei, A.-S., Jezberová, J., Seďa, J., Rychtecký, P., Znachor, P., Šimek, K., Ghai, R., 2023. *High-resolution metagenomic reconstruction of the freshwater spring bloom*. Microbiome 11, 15.
https://doi.org/10.1186/s40168-022-01451-4

Lapoussière, A., Michel, C., Starr, M., Gosselin, M., Poulin, M., 2011. *Role of free-living and particle-attached bacteria in the recycling and export of organic material in the Hudson Bay system*. J. Marine Syst. 88, 434–445.
https://doi.org/10.1016/j.jmarsys.2010.12.003

Lim, E.L., Dennett, M.R., Caron, D.A., 1999. *The ecology of Paraphysomonas imperforata based on studies employing oligonucleotide probe identification in coastal water samples and enrichment cultures*. Limnol. Oceanogr. 44, 37–51.
https://doi.org/10.4319/lo.1999.44.1.0037

Logares, R., Lindstrom, E.S., Langenheder, S., Logue, J.B., Paterson, H., Laybourn-Parry, J., Rengefors, K., Tranvik, L., Bertilsson, S., 2013. *Biogeography of bacterial communities exposed to progressive long-term environmental change*. ISME J. 7, 937–948.
https://doi.org/10.1038/ismej.2012.168

Lopez-Garcia, P., Rodriguez-Valera, F., Pedros-Alio, C., Moreira, D., 2001. *Unexpected diversity of small eukaryotes in deep-sea Antarctic plankton*. Nature 409, 603–607.
https://doi.org/10.1038/35054537

Ludwig, W., Strunk, O., Westram, R., Richter, L., Meier, H., Yadhukumar, Buchner, A., Lai, T., Steppi, S., Jobb, G., Forster, W., Brettske, I., Gerber, S., Ginhart, A.W., Gross, O., Grumann, S., Hermann, S., Jost, R., Konig, A., Liss, T., Lussmann, R., May, M., Nonhoff, B., Reichel, B., Strehlow, R., Stamatakis, A., Stuckmann, N., Vilbig, A., Lenke, M., Ludwig, T., Bode, A., Schleifer, K.H., 2004. *ARB: a software environment for sequence data*. Nucleic Acids Res. 32, 1363–1371.
https://doi.org/10.1093/nar/gkh293

Mangot, J.F., Lepere, C., Bouvier, C., Debroas, D., Domaizon, I., 2009. *Community structure and dynamics of small eukaryotes targeted by new oligonucleotide probes: new insight into the lacustrine microbial food web*. Appl. Environ. Microbiol. 75, 6373–6381.
https://doi.org/10.1128/AEM.00607-09

Massana, R., Gobet, A., Audic, S., Bass, D., Bittner, L., Boutte, C., Chambouvet, A., Christen, R., Claverie, J.-M., Decelle, J., Dolan, J., Dunthorn, M., Edvardsen, B., Forn, I., Forster, D., Guillou, L., Jaillon, O., Kooistra, W., Logares, R., de Vargas, C., 2015. *Marine protist diversity in European coastal waters and sediments as revealed by high-throughput sequencing*. Environ. Microbiol. 17, 4035–4049.
https://doi.org/10.1111/1462-2920.12955

Massana, R., Guillou, L., Diez, B., Pedros-Alio, C., 2002. *Unveiling the Organisms behind Novel Eukaryotic Ribosomal DNA Sequences from the Ocean*. Appl. Environ. Microbiol. 68, 4554–4558.
https://doi.org/10.1128/AEM.68.9.4554-4558.2002

Massana, R., Guillou, L., Terrado, R., Forn, I., Pedros-Alio, C., 2006a. *Growth of uncultured heterotrophic flagellates in unamended seawater incubations*. Aquat. Microb. Ecol. 45, 171–180.
https://doi.org/10.3354/ame045171

Massana, R., Terrado, R., Forn, I., Lovejoy, C., Pedros-Alio, C., 2006b. *Distribution and abundance of uncultured heterotrophic flagellates in the world oceans*. Environ. Microbiol. 8, 1515–1522.
https://doi.org/10.1111/j.1462-2920.2006.01042.x

Mazur-Marzec, H., Andersson, A.F., Błaszczyk, A., Dąbek, P., Górecka, E., Grabski, M., Jankowska, K., Jurczak-Kurek, A., Kaczorowska, A.K., Kaczorowski, T., Karlson, B., Kataržytė, M., Kobos, J., Kotlarska, E., Krawczyk, B., Łuczkiewicz, A., Piwosz, K., Rybak, B., Rychert, K.,

Sjöqvist, C., Surosz, W., Szymczycha, B., Toruńska-Sitarz, A., Węgrzyn, G., Witkowski, A., Węgrzyn, A., 2024. *Biodiversity of microorganisms in the Baltic Sea: the power of novel methods in the identification of marine microbes*. FEMS Microbiol. Rev. 48(5), fuae024. https://doi.org/10.1093/femsre/fuae024

Minh, B.Q., Schmidt, H.A., Chernomor, O., Schrempf, D., Woodhams, M.D., von Haeseler, A., Lanfear, R., 2020. *IQ-TREE 2: New Models and Efficient Methods for Phylogenetic Inference in the Genomic Era*. Mol. Biol. Evol. 37, 1530–1534. https://doi.org/10.1093/molbev/msaa015

Moon-van der Staay, S.Y., De Wachter, R., Vaulot, D., 2001. *Oceanic 18S rDNA sequences from picoplankton reveal unsuspected eukaryotic diversity*. Nature 409, 607–610. https://doi.org/10.1038/35054541

Mukherjee, I., Grujčić, V., Salcher, M.M., Znachor, P., Seďa, J., Devetter, M., Rychtecký, P., Šimek, K., Shabarova, T., 2024. *Integrating depth-dependent protist dynamics and microbial interactions in spring succession of a freshwater reservoir*. Environ. Microbiome 19, 31. https://doi.org/10.1186/s40793-024-00574-5

Mukherjee, I., Hodoki, Y., Nakano, S.-i., 2015. *Kinetoplastid flagellates overlooked by universal primers dominate in the oxygenated hypolimnion of Lake Biwa, Japan*. FEMS Microbiol. Ecol. 91, fiv083. https://doi.org/10.1093/femsec/fiv083

Mukherjee, I., Salcher, M.M., Andrei, A.-Ş., Kavagutti, V.S., Shabarova, T., Grujčić, V., Haber, M., Layoun, P., Hodoki, Y., Nakano, S.-i., Šimek, K., Ghai, R., 2020. *A freshwater radiation of diplonemids*. Environ. Microbiol. 22, 4658–4668. https://doi.org/10.1111/1462-2920.15209

Piwosz, K., 2019. *Weekly dynamics of abundance and size structure of specific nanophytoplankton lineages in coastal waters (Baltic Sea)*. Limnol. Oceanogr. 64, 2172–2186. https://doi.org/10.1002/lno.11177

Piwosz, K., Całkiewicz, J., Gołębiewski, M., Creer, S., 2018. *Diversity and community composition of pico- and nanoplanktonic protists in the Vistula River estuary (Gulf of Gdańsk, Baltic Sea)*. Estuar. Coast. Shelf Sci. 207, 242–249. https://doi.org/10.1016/j.ecss.2018.04.013

Piwosz, K., Kownacka, J., Ameryk, A., Zalewski, M., Pernthaler, J., 2016. *Phenology of cryptomonads and the CRY1 lineage in a coastal brackish lagoon (Vistula Lagoon, Baltic Sea)*. J. Phycol. 52, 626–637. https://doi.org/10.1111/jpy.12424

Piwosz, K., Mukherjee, I., Salcher, M.M., Grujčić, V., Šimek, K., 2021. *CARD-FISH in the Sequencing Era: Opening a New Universe of Protistan Ecology*. Front. Microbiol. 12, 640066. https://doi.org/10.3389/fmicb.2021.640066

Piwosz, K., Pernthaler, J., 2010. *Seasonal population dynamics and trophic role of planktonic nanoflagellates in coastal surface waters of the Southern Baltic Sea*. Environ. Microbiol. 12, 364–377. https://doi.org/10.1111/j.1462-2920.2009.02074.x

Piwosz, K., Pernthaler, J., 2011. *Enrichment of omnivorous cercozoan nanoflagellates from coastal Baltic Sea waters*. PLoS ONE 6, e24415. https://doi.org/10.1371/journal.pone.0024415

Piwosz, K., Shabarova, T., Pernthaler, J., Posch, T., Šimek, K., Porcal, P., Salcher, M.M., 2020. *Bacterial and eukaryotic small-subunit amplicon data do not provide a quantitative picture of microbial communities, but they are reliable in the context of ecological interpretations*. mSphere 5, e00052-00020. https://doi.org/10.1128/msphere.00052-20

Santoferrara, L., Burki, F., Filker, S., Logares, R., Dunthorn, M., McManus, G.B., 2020. *Perspectives from Ten Years of Protist Studies by High-Throughput Metabarcoding*. J. Eukaryot. Microbiol. 67, 612–622. https://doi.org/10.1111/jeu.12813

Schoenle, A., Hohlfeld, M., Hermanns, K., Mahé, F., de Vargas, C., Nitsche, F., Arndt, H., 2021. *High and specific diversity of protists in the deep-sea basins dominated by diplonemids, kinetoplastids, ciliates and foraminiferans*. Commun. Biol. 4, 501. https://doi.org/10.1038/s42003-021-02012-5

Steenwyk, J.L., Buida, T.J., 3rd, Li, Y., Shen, X.-X., Rokas, A., 2020. it ClipKIT: A multiple sequence alignment trimming software for accurate phylogenomic inference. PLoS Biol. 18, e3001007. https://doi.org/10.1371/journal.pbio.3001007

Strom, L.S., Morello, T.A., Kelley, J.B., 1998. *Protozoan size influences algal pigment degradation during grazing*. Mar. Ecol. Prog. Ser. 164, 189–197.

Tedersoo, L., Hosseyni Moghaddam, M.S., Mikryukov, V., Hakimzadeh, A., Bahram, M., Nilsson, R.H., Yatsiuk, I., Geisen, S., Schwelm, A., Piwosz, K., Prous, M., Sildever, S., Chmolowska, D., Rueckert, S., Skaloud, P., Laas, P., Tines, M., Jung, J.-H., Choi, J.H., Alkahtani, S., Anslan, S., 2024. *EUKARYOME: the rRNA gene reference database for identification of all eukaryotes*. Database 2024, baae043. https://doi.org/10.1093/database/baae043

Telesh, I., Schubert, H., Skarlato, S., 2013. *Life in the salinity gradient: Discovering mechanisms behind a new biodiversity pattern*. Estuar. Coast. Shelf Sci. 135, 317–327. https://doi.org/10.1016/j.ecss.2013.10.013

Telesh, I.V., Schubert, H., Skarlato, S.O., 2011. *Revisiting Remane's concept: evidence for high plankton diversity and a protistan species maximum in the horohalinicum of the Baltic Sea*. Mar. Ecol. Prog. Ser. 421, 1–11. https://doi.org/10.3354/meps08928

Thompson, L.R., Sanders, J.G., McDonald, D., Amir, A., Ladau, J., et al., *A communal catalogue reveals Earth's multi-*

scale microbial diversity. Nature 551, 457–463. https://doi.org/10.1038/nature24621

Vaulot, D., Geisen, S., Mahé, F., Bass, D., 2022. *pr2-primers: An 18S rRNA primer database for protists*. Mol. Ecol. Resour. 22, 168–179. https://doi.org/10.1111/1755-0998.13465

Villarino, E., Watson, J.R., Jönsson, B., Gasol, J.M., Salazar, G., Acinas, S.G., Estrada, M., Massana, R., Logares, R., Giner, C.R., Pernice, M.C., Olivar, M.P., Citores, L., Corell, J., Rodríguez-Ezpeleta, N., Acuña, J.L., Molina-Ramírez, A., González-Gordillo, J.I., Cózar, A., Martí, E., Cuesta, J.A., Agustí, S., Fraile-Nuez, E., Duarte, C.M., Irigoien, X., Chust, G., 2018. *Large-scale ocean connectivity and planktonic body size*. Nat. Commun. 9, 142. https://doi.org/10.1038/s41467-017-02535-8

Weber, F., Anderson, R., Foissner, W., Mylnikov, A.P., Jürgens, K., 2014. *Morphological and molecular approaches reveal highly stratified protist communities along Baltic Sea pelagic redox gradients*. Aquat. Microb. Ecol. 73, 1–16. https://doi.org/10.3354/ame01702

Witek, Z., Ochocki, S., Maciejowska, M., Pastuszak, M., Nakonieczny, J., Podgorska, B., Kownacka, J.M., Mackiewicz, T., Wrzesinska-Kwiecien, M., 1997. *Phytoplankton primary production and its utilization by the pelagic community in the coastal zone of the Gulf of Gdańsk (southern Baltic)*. Mar. Ecol. Prog. Ser. 148, 169–186. https://doi.org/10.3354/meps148169

Worden, A.Z., Follows, M.J., Giovannoni, S.J., Wilken, S., Zimmerman, A.E., Keeling, P.J., 2015. *Rethinking the marine carbon cycle: Factoring in the multifarious lifestyles of microbes*. Science 347, 1257594. https://doi.org/10.1126/science.1257594

Wylezich, C., Herlemann, D.P.R., Jürgens, K., 2018. *Improved 18S rDNA amplification protocol for assessing protist diversity in oxygen-deficient marine systems*. Aquat. Microb. Ecol. 81, 83–94. https://doi.org/10.3354/ame01864

Wylezich, C., Juergens, K., 2011. *Protist diversity in suboxic and sulfidic waters of the Black Sea*. Environ. Microbiol. 13, 2939–2956. https://doi.org/10.1111/j.1462-2920.2011.02569.x

Zillén, L., Conley, D.J., Andrén, T., Andrén, E., Björck, S., 2008. *Past occurrences of hypoxia in the Baltic Sea and the role of climate variability, environmental change and human impact*. Earth-Sci. Rev. 91, 77–92. https://doi.org/10.1016/j.earscirev.2008.10.001